Multiphase Flow Characterized by Scattering of Ultrasound

Johan Carlson*, Anders Grennberg†, and Jerker Delsing*
*Luleå University of Technology, Div. of Industrial Electronics, SE-971 87 Luleå, Sweden
†Luleå University of Technology, Div. of Signal Processing, SE-971 87 Luleå, Sweden

Abstract— **In this paper, we present and verify a simple mathematical model of the scattering of ultrasound by particles in a multiphase flow.**

We show that a *line-of-sight* model can be used to describe how the multi-path propagation of ultrasound in a dilute suspension of glass spheres and water affects the waveform. Simulation results agree with measured data for particle concentrations up to 3 per cent.

Furthermore, the simulations and experiments indicate that there are two main effects affecting the signal waveform; the shadowing of the direct wave between transmitter and receiver, and multi-path propagation. For small particles, the multi-path propagation is the largest effect, while the attenuation of the direct wave increases for larger particles. We see that the multi-path propagation affects the tail of the pulse, while the attenuation of the direct wave mainly affects the first two maxima. The relationship between these two effects can therefore be used to characterize a multiphase suspension.

I. Introduction

The long-term goal of our project is to develop a non-invasive multiphase flow metering methodology for measuring bulk flow velocity, mass fractions, and mass fraction velocities in dilute multiphase flows. Important areas of application are, oil and gas, paper pulp, and mining industry. A good overview of what has been done in this area can be found in the book by Chaoki, *et al.* [1] and in the review article by Whitaker [2]. Our basic idea is to use some established method for measuring the bulk flow velocity (see for example the sing-around flow meter described in [3]), and then use through-transmission ultrasound to determine mass fractions and mass fraction velocities. In this paper, we characterize a multiphase flow by examining how scattering affects the received signal waveform.

When transmitting ultrasound through a multiphase medium containing solid particles, the sound waves are scattered and attenuated. In this paper, we present and verify a mathematical model that qualitatively describes how scattering affects the waveform of ultrasonic pulses. The idea behind the model is that the received ultrasonic signal can be written as the sum of a direct wave between the transmitter and the receiver, and scattered waves.

II. The Multi-path Propagation Model

Under certain conditions, scattering occurs when sound waves are obstructed by particles. As a rule of thumb (see for example [4], chapter 8) we can assume that scattering occurs if the condition in equation (1) is satisfied.

$$\frac{2\pi}{\lambda}a \gg 1, \tag{1}$$

where λ is the wavelength of the sound and a is the radius of the scattering particle.

Since the theory of scattering is very complex, we will derive a simplified mathematical model, that qualitatively describes the effect of scattering on the waveform of a received ultrasonic pulse. Figure 1 illustrates the general idea of the *line-of-sight* scattering model.

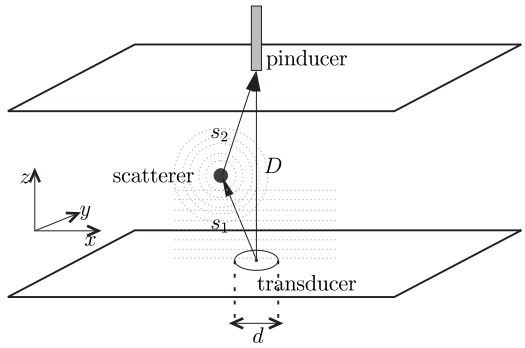

Figure 1 – *Line-of-sight* model for single scattering by a spherical particle.

Assume that waves transmitted from the transducer are scattered by N spherical particles as in figure 1. In this case the received pulse, $y(t)$, can be regarded as the sum of delayed and attenuated versions of the

transmitted pulse, $p(t)$. Equation (2) is a mathematical representation of this idea

$$y(t) = \alpha_0 p(t) + \sum_{n=1}^{N} \alpha_n p(t - \tau_n), \tag{2}$$

where α_0 is the attenuation of the direct wave, $\{\alpha_1, \alpha_2, \ldots, \alpha_N\}$ is the attenuation coefficients for the N scatterers, $p(t)$ is the transmitted pulse, and τ_n is the time delay corresponding to the increase in distance caused by scatterer n. The attenuation coefficients depend on several factors, for example the position of the scatterer and the relationship between wavelength and particle size.

We assume that a particle will affect the received signal if it is located somewhere in the cylinder with the tranmitting transducer as base, and with height D (as defined in figure 1). Figure 2 supports this, since we see that most of the received energy is located in that region.

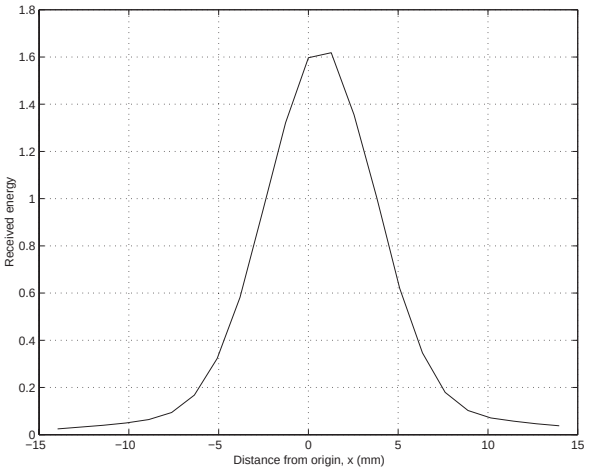

Figure 2 – Received energy in the region around the origin, measured in pure water. The diameter of the transmitting transducer was 14 mm, and the distance between transmitter and receiver was 145 mm.

If particle n is located at (x_n, y_n, z_n) somewhere in this volume, the propagation distance $s_1 + s_2$ can be expressed as

$$s_n = \sqrt{x_n^2 + y_n^2 + z_n^2} + \sqrt{x_n^2 + y_n^2 + (D - z_n)^2} \tag{3}$$

where we for simplicity assume that x_n and y_n are uniformly distributed over the interval $\left[-\frac{d}{2}, \frac{d}{2}\right]$ and that z_n is uniformly distributed over the interval $[0, D]$.

Using the distances s_n from equation (3), we obtain the corresponding time delays τ_n as

$$\tau_n = \frac{s_n(x_n, y_n, z_n) - D}{v} \tag{4}$$

where v is the speed of sound and D is the propagation distance of the direct wave.

For different relationships between particle size and wavelength, the energy is scattered differently in space. For simplicity we assume that the energy spreads spherically from the scatterer. We also assume the no energy is absorbed by the scatterer. Thus, the attenuation coefficient for each scattered pulse can be approximated to be

$$\alpha_n = \frac{K_2}{s_{n2}^2}, n \geq 1 \tag{5}$$

where s_{n2} is the distance between the n:th scatterer and the receiver and K_2 is some constant (to be determined experimentally). If no particles shadow the direct wave between transmitter and receiver, the attenuation of the direct wave is generally very small compared to the attenuation of the scattered waves. There are cases, however, when no direct wave is present, because some particles shadow the propagation path.

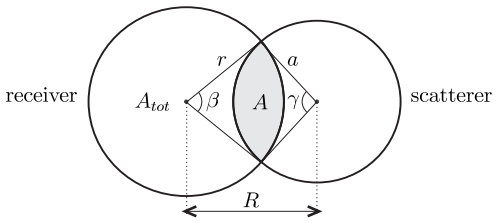

Figure 3 – Situation where a scatterer shadows the receiver.

In order to keep the model simple, we assume that the amount of received energy is proportional to the area of the receiver which is not shadowed. This leads to the following expression for α_0.

$$\alpha_0 = K_0 \left(1 - K_1 \frac{A}{A_{tot}}\right), \tag{6}$$

where K_0 is a constant corresponding to the attenuation of an undisturbed wave, K_1 is a constant corresponding to the amount of energy lost by shadowing, and A/A_{tot} is the ratio of the shadow to the receiver area. If there is only one scatterer shadowing the receiver, we have the case illustrated in figure 3. If the scatterer and the receiver partially overlaps, that is $\min(r, a) < R < r + a$, the area of the intersection, A, is given by

$$A = \frac{r^2}{2}(\beta - \sin\beta) + \frac{a^2}{2}(\gamma - \sin\gamma). \tag{7}$$

where, by the law of cosines,

$$\beta = 2\cos^{-1}\left(\frac{r^2 + R^2 - a^2}{2aR}\right) \tag{8}$$

$$\gamma = 2\cos^{-1}\left(\frac{a^2 + R^2 - r^2}{2aR}\right) \tag{9}$$

If, however, the receiver is totally shadowed or, if the scatterer is smaller than the receiver, we have a maximum shadowing area, given by

$$A = [\min(a, r)]^2 \cdot \pi \tag{10}$$

If there are more than one scatterer shadowing the receiver, the expression for A, becomes more complicated. For simplicity we sum the contributions of each scatterer, making sure that the total shadowed area is not greater than the receiver area.

III. Experiments

In this section, we first describe the experimental setup and the equipment we used, followed by a brief description of the analysis tools used to process the collected data. Finally, we describe how the computer simulations of the model in section II was made.

A. Experimental Setup

In order to verify the model, we prepared suspensions of glass spheres and water. The glass spheres had an average radius of 1 mm, which, according to equation (1), should be enough for scattering to be present, since the transmitting transducer had a center frequency of 3 MHz. The outer diameter of the transducer was 14 mm. We prepared suspensions with concentrations of 1, 2, and 3 per cent (by volume). The suspensions were enclosed in the suspension tank depicted in figure 4.

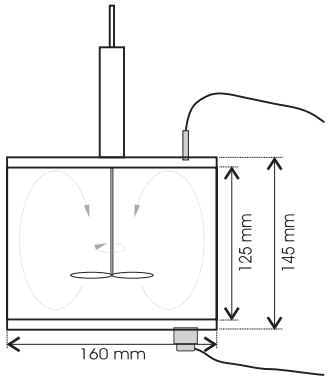

Figure 4 – Suspension tank used in the experiments.

The receiver was a VP-1093 pinducer[1] with a 10 MHz input bandwidth and a crystal radius of 1 mm. The receiver and transmitter was centered.

For each concentration, 100 pulses were measured. We noticed that there were small time delays between the recorded pulses. We found that some of these delays came from triggering of the sampling equipment, and by increasing the sampling frequency this effect became smaller. We also found that when we increased the speed of the stirring equipment, the vibrations in the system increased. This may also cause time delays, since the distance between transmitter and receiver could change. If the observed time delays are the result of experimental errors, they have to be estimated and compensated for.

[1]The VP-1093 pinducer was manufactured by Valpey-Fisher Corp., 75 South Street, Hopkinton, MA 01748.

B. Estimating Time Delays

Whether or not the observed time delays were the result of experimental errors, they have to be estimated. To accomplish this, we used the algorithm by Grennberg and Sandell, presented in [5]. This is a more efficient method than an ordinary cross-correlation method, especially for estimating small time delays between narrowband pulses.

C. Sensitivity to Vibrations

In order to determine if the time shifts between recorded pulses were the results of mechanical disturbances, such as vibrations, we first estimated the time delays with respect to the first recorded pulse. Figure 5 shows the resulting histogram of the delays.

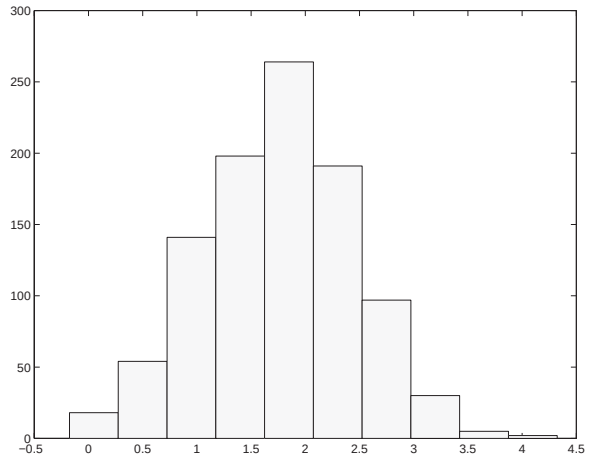

Figure 5 – Distribution of estimated time delays, measured in water.

We note that the delays looks like they originate from a normal distribution. However, if the delays were due to mechanical disturbances, we would expect them to have zero mean. The observed bias can be explained by the fact that we estimated the delays relative to the first recorded pulse, and not to an *exact* measurement.

Now, if we assume that the delays are samples from a normal distribution with mean μ and standard deviation σ, a 95 per cent confidence interval can be calculated. Since the mean and standard deviation are

unknown, we first estimated these, using equations (11) and(12).

$$\widehat{\mu} = \frac{1}{N}\sum_{n=1}^{N}\theta_n, \tag{11}$$

$$\widehat{\sigma} = \left[\frac{1}{N-1}\sum_{n=1}^{N}(\theta_n-\widehat{\mu})^2\right]^{1/2}. \tag{12}$$

The corresponding precision limits are then given by(see [6])

$$P_\theta = t_{N-1}\cdot\widehat{\sigma}, \tag{13}$$

$$P_{\widehat{\mu}} = t_{N-1}\frac{\widehat{\sigma}}{\sqrt{N}}, \tag{14}$$

where the t-distribution is used because $\widehat{\sigma}$ was estimated.

This means that, with 95 per cent probability, the $[-P_\theta - P_{\widehat{\mu}}, P_\theta + P_{\widehat{\mu}}]$ will enclose the time delays.

To see whether or not the time delay corresponding to the precision limit $P_\theta + P_{\widehat{\mu}}$ is likely to come from vibrations, we calculated the change in distance between the transmitter and receiver this would require. The sampling time was $2\cdot10^{-9}$s and the speed of sound in water is around 1480 m/s. For the measurements shown in figure 5 the upper precision limit was determined to be 1.39 samples. Equation (15) gives the corresponding change in distance, ds.

$$\begin{aligned} ds &= (P_\theta + P_{\widehat{\mu}})\cdot T_s\cdot v = \\ &= 1.39\cdot 2\cdot 10^{-9}\cdot 1480 \approx 4.0\ \mu m \end{aligned} \tag{15}$$

For the case with 3 per cent particle concentration, the corresponding distance would be 20 μm, assuming all time shifts come from distance changes.

As we see, the distance change required to cause these time delays is very small, and we conclude that it certainly could come from vibrations and other mechanical disturbances in the system. When we increased the particle concentration, we had to use a higher rotation speed, causing more vibrations. If we average the measured pulses directly, the time delays cause the signal waveform to be distorted.. Therefore, we first shift all measured pulses according to the estimated time delays, by using Lagrange's interpolation formula.

IV. Results

After measuring all pulses, we simulated 100 pulses for each concentration. Based on the concentration, the position of a number of particles was generated, assuming that the particles were uniformly distributed in the sample volume. As input pulse to the model, we used an average pulse taken from measurements in pure water. The parameters, K_0, K_1, and K_2 in the model

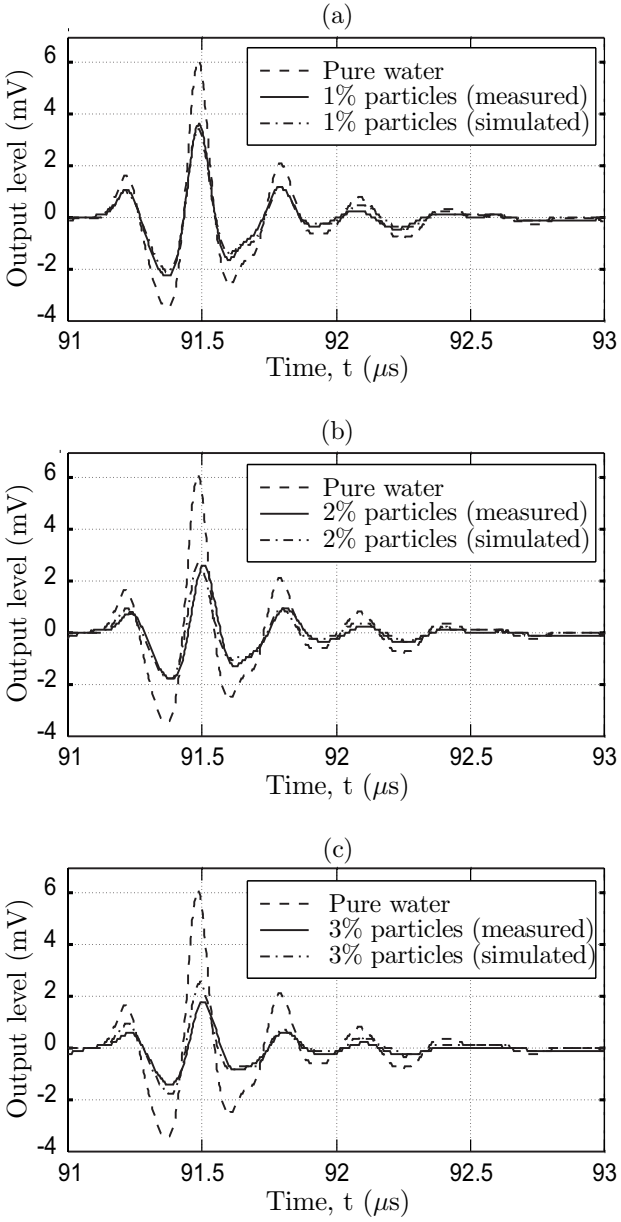

Figure 6 – Comparison of averaged pulses.

described in section II. was then adjusted so that the average pulses from the measurements and simulations fit for the suspension with 1 per cent of glass spheres. We then performed simulations for the other concentrations, but without changing any parameters in the model. Figure 6(a) shows the resulting average pulse after adjusting the model parameters. Figure 6(b) and (c) show how the model follows when concentration was increased to 2 and 3 per cent, respectively. In this case the model parameters were set as $K_0 = 0.8$, $K_1 = 0.5$, and $K_2 = 6.5\cdot10^{-5}$. These values were chosen so that the model output and the measured pulses agree for 1

per cent of glass spheres.We see that the agreement is very good for 1 and 2 per cent, but slightly worse for 3 per cent of glass spheres. When deriving the model, we assumed that the sound is only scattered once during the propagation. When the concentration of particles increases, this assumption does no longer hold, and this could be what we see in figure 6(c).

Figure 6 shows that the simulated signal waveform agrees with measured data, and in figure 7 we see that the average energy of the simulated pulses also agrees with measured data.

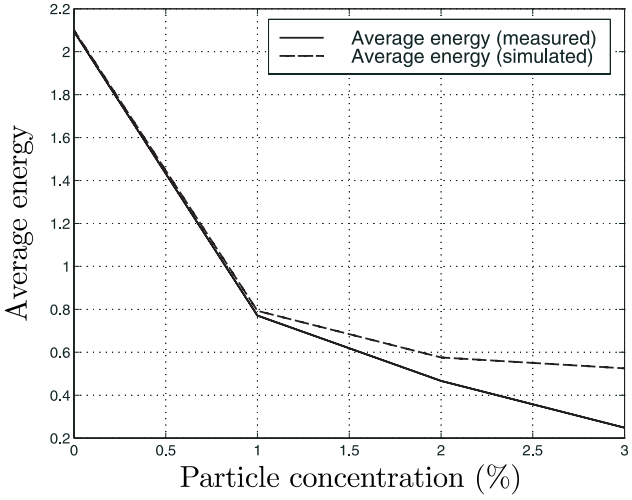

Figure 7 – Average energy for measured and simulated pulses.

V. Conclusions

From the simulations we conclude that this model can be used to qualitatively describe the effect of scattering of ultrasound for this experimental setup. It is clear that the main effect is the shadowing of the direct wave between the transmitter and the receiver. The multi-path propagation is also significant to the change of waveform, and we can see that when scattering occurs, the variations in pulse energy increase towards the end of the pulse. For large particles, the shadowing of the direct wave is the main effect, while for smaller particles, the multi-path propagation increases, causing larger variations at the tail of the pulses. Thus, by studying the waveform of a received ultrasonic pulse, we can determine whether or not scattering has occurred, and by that draw conclusions about the particle size and attenuation. If the model is developed further, it is possible that the relationship between the damping of the first two maxima of the pulse and the increase of energy in the tail of the pulse can be used to determine volume fractions.

We also see from the simulations that the assumption that the sound is scattered only once, only holds for low particle concentrations.

References

[1] J. Chaoki, L. Larachi, and M. P. Dudoković, *Non-Invasive Monitoring of Multiphase Flows*. Elsevier, 1997.

[2] T. S. Whitaker, "A review of multiphase flowmeters and future development potential," in *Flow Measurement: Proceedings of the 6th Int. Conf. on Flow Measurement, FLOMEKO'93*, (Seoul, Korea), pp. 628–634, Oct. 1993.

[3] J. Delsing, "A new velocity algorithm for sing-around type flow meters," *IEEE Trans. on Ultrasonics, Ferroelectrics, and Frequency Control*, vol. 34, no. 4, pp. 431–436, 1987.

[4] P. M. Morse and K. U. Ingaard, *Theoretical Acoustics*. Princeton University Press, 1986.

[5] A. Grennberg and M. Sandell, "Estimation of subsample time delay differences in narrowband ultrasonic echoes using the hilbert transform correlator," *IEEE Trans. on Ultrasonics, Ferroelectrics, and Frequency Control*, vol. 41, pp. 588–595, sep 1994.

[6] H. W. Coleman and W. G. Steele Jr., *Experimentation and Uncertainty Analysis for Engineers*. Wiley Interscience, 1989.